Kidney International, Vol. 13 (1978), pp. 344–360

Physicochemical aspects of urolithiasis

BIRDWELL FINLAYSON

Division of Urology, Department of Surgery, University of Florida, College of Medicine, Gainesville, Florida

The following discussion centers on calcium oxalate and calcium phosphate stones, but permits generalization to other forms of stone. Although it constitutes a primer on the subject, it does attempt to deal with inconsistencies in our current meager knowledge of the physical characteristics of urolithiasis. In addition, it describes concepts and approaches that appear to be useful and that should be incorporated into urolithiasis research, to make future work in the field susceptible to analysis by conventional physical theory.

The known physicochemical features of urolithiasis are readily divided into four interrelated subjects: the driving force (supersaturation), nucleation, the growth of crystals and particles, and aggregation.

The chemical driving force, urinary supersaturation

Supersaturation of urine with respect to the salts that stones will or do consist of gives rise to the thermodynamic driving force for the formation of stones. This driving force, expressed as free energy (ΔG), is given by

$$\Delta G = RT \ln \left(\frac{A_i}{A_o} \right), \qquad (1)$$

where R is the gas constant, T is the temperature, and A_i and A_o are the activities of the unionized salt species in solution at any given condition and at equilibrium, respectively [1]. Activity (A) is related to concentration (C) through an activity coefficient (f) by

$$A = fC. \qquad (2)$$

When urine is such that, for a given stone salt, $A_i/A_o < 1$, then $\Delta G < 0$, the urine is said to be *undersaturated* with respect to the stone salt, and any stones that are present can dissolve [2, 3]. As an example, treatment with allopurinol causes A_i/A_o to be less than 1 with respect to uric acid, and it is common for uric acid stones to dissolve in this circumstance. When urine is such that, for a given stone salt, $A_i/A_o = 1$, then $\Delta G = 0$, and the urine is said to be *saturated*. In this circumstance, old stones will not dissolve, and new ones will not form; but old stones can grow, in the sense that aggregation of pre-existing stones can occur. When, for a given stone salt, $A_i/A_o > 1$, then $\Delta G > 0$, and the urine is said to be *supersaturated*. In this circumstance, there is available free energy; if stones are present, they may grow, but if stone crystals are not present, then precipitation will not occur, unless A_i/A_o exceeds an experimentally ill-defined limit called the "metastable limit." Above the metastable limit, it is possible both for new stones to form and for old stones to grow (Fig. 1).

Inasmuch as the progress of stone disease is governed by the available free energy, it is important to have a quantitative measure of A_i/A_o; it makes it possible to identify people who have an increased likelihood of stone disease and to monitor the effectiveness of the anti-stone therapies that operate by reducing A_i/A_o, such as magnesium oxide, hydrochlorothiazide, and cellulose phosphate. In principle, there are a variety of methods for measuring A_i/A_o, but during the last 10 years only three have received persistent attention. Calculation of A_i/A_o was popularized by Robertson [4]. Pak and Chu [5] have described a semi-empirical equilibration technique that capitalizes on the linear relations among the urinary concentrations of calcium, phosphate, and oxalate. In general, the relations used by Pak and Chu are nonlinear; but in the range of change encountered during calcium oxalate or calcium phosphate precipitation in urine, the expected error of a linear assumption is less than 2%, as judged by the *ab initio* calculations. Gill, Silvert, and Roma have introduced a radionuclide tracer into the Pak method, to simplify chemical quantitation [6]. With a firm grasp of the *ab initio* calculations, a theoretical understanding of the methods of Pak and Gill will appear elementary.

0085–2538/78/0013–0344 $03.40

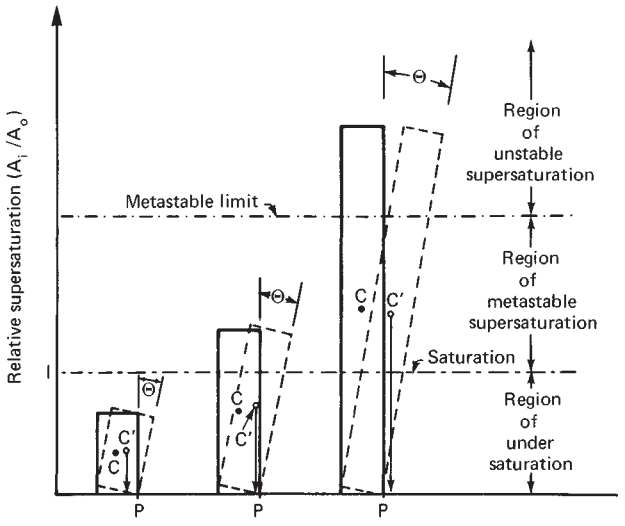

Fig. 1. *A mechanical analogy of chemical metastability.* The *vertical bars* represent concentrations of a precipitable salt. The available thermal free energy is sufficient to cause fluctuations that tip the bars about the pivot point (P) through angular displacement (θ). When the center of mass (C) is displaced (C′) lateral to P, the mechanical bar will fall over, which is equivalent to precipitation. In the region of undersaturation, the bar cannot be toppled by fluctuations equal to θ. In the region of metastable supersaturation, catalytic surfaces can augment the fluctuations so that C′ is displaced lateral to P. This case is equivalent to crystal growth or heterogeneous nucleation. In the region of unstable supersaturation, thermal concentration fluctuations, θ, are sufficient to place C′ lateral to P and cause the bar to fall over, which is analogous to spontaneous precipitation.

Ab initio calculations of A_i/A_o. Urine is a solution containing a set of cations ($\vec{C}$) and a set of anions ($\vec{A}$). Some of the cations and anions will very rapidly (relaxation time, $\sim 10^{-6}$ sec) undergo ion complex formation

$$C_k + A_j \overset{K_{k,j}}{\rightleftarrows} CA_{k,j}. \qquad (3)$$

For each complex formed, the equilibrium is governed by the mass action relation,

$$K_{k,j} = [CA_{k,j}]f_{k,j}/[C_k][A_j]f_k f_j, \qquad (4)$$

where $K_{k,j}$ is the stability constant for the $(k,j)^{th}$ complex, f_n is the activity coefficient for the n^{th} charged species, and brackets indicate concentration. If $[TC_k]$ is the sum of the concentrations of all species containing C_k, then conservation of mass requires that

$$[TC_k] = [C_j] + \sum_{j=1}^{mc} [CA_{k,j}]n_{k,j,k} \qquad (5a)$$

and

$$[TA_j] = [A_j] + \sum_{k=1}^{ma} [CA_{k,j}]n_{k,j,j}. \qquad (5b)$$

In Equations 5a and 5b, m is the number of possible complexes, and $n_{k,j,l}$ is the stoichiometric number of the l^{th} species in the $(k,j)^{th}$ complex. The stoichiometric number is required for polynuclear complexes, such as $Ca_2C_2O_4^{2-}$. Equation 5a transforms to

$$[C_k] = [TC_k]/(1 + \Sigma[CA_{k,j}]n_{k,j,k}). \qquad (6)$$

Equation 5b undergoes a similar transformation. Equations of the genre of Equation 4 can be substituted into Equations 5a and 5b, giving a set of nonlinear simultaneous equations in $[TC_k]$, $[TA_j]$, $[C_k]$, and $[A_j]$, whose solution rapidly converges to self-consistency by iterative approximation. In my laboratory, it was found empirically that in most urines the activity coefficient, f_Z, can be taken to be 0.73^{Z^2}, with Z being the electronic charge of the species in question. Alternatively, f_Z at 38°C can be calculated with

$$f_Z = \exp(-1.202Z^2((\sqrt{w}/(1+\sqrt{w}))-0.285w)). \qquad (7)$$

Equation 7 is the Davies modification of the Guggenheim approximation of the Debye-Hückel first-order solution of the Poisson-Boltzman equation for the energy of the electrostatic field of an ion in ionic solution [2], in which w is the ionic strength given by

$$2w = \sum_{k=1}^{V} [C_k](Z_k)^2 + \sum_{j=1}^{U} [A_j](Z_j)^2 + \sum_{k=j=1}^{R\ S} [CA_{k,j}](Z_{k,j})^2, \qquad (8)$$

with R, S, U, and V as the numbers of the species being summed. In practice, to make an *ab initio* calculation, urine is analyzed for pH and total sodium, potassium, calcium, magnesium, ammonium, sulfate, phosphate, citrate, oxalate, urate, and chloride, and the calculation is made with Equations 5–8. There are far too many equations to attempt such a calculation for urine by hand. A number of computer programs, however, have been written and can be obtained from their authors[a–d]. (The interested reader will find a step-by-step guide through the *ab initio* calculation presented elsewhere [7]).

Working with urine at 25°C, Robertson [4] showed a high degree of correlation between *ab initio* calcu-

[a] G. Nancollas, Department of Chemistry, New York University at Buffalo, Buffalo, New York.
[b] W.G. Robertson, MRC Unit, Leeds, Great Britain.
[c] J. Meyer, National Institute of Dental Research, Building 30, Room 211, Bethesda, Maryland 20014.
[d] The Royal Institute of Technology, Department of Inorganic Chemistry, Stockholm, Sweden. Ask for LETAGROP and HALTAFALL.

lated and experimentally measured calcium concentration, $[Ca^{2+}]$. Robertson's early *ab initio* calculations used an inappropriate stability constant for calcium oxalate that necessarily gave an appreciable error in the calculated activity of $A_i(CaC_2O_4)$. But approximately the same fractional error occurs in the calculated value of $A_o(CaC_2O_4)$; thus, whenever Robertson's calculations for calcium oxalate are presented as A_i/A_o (i.e., relative supersaturation), the estimates are reasonable from a theoretical point of view. In recent calculations, Robertson et al has used a calcium oxalate stability constant of 1,900 M^{-1} [8]. It is not clear whether his current program has been altered for 38°C. In my laboratory, using a 38°C program and a calcium oxalate stability constant of 2,746 M^{-1} [9], we are able to calculate the equilibrium value of calcium oxalate precipitating from artificial urine to within 20%. *Ab initio* calculations of A_i/A_o for whewellite do not agree well with the results of the semi-empirical methods to be discussed later; however, if for no other reason, *ab initio* calculations are useful because they provide an incisive technique for investigating the semi-empirical methods.

In an effort to reduce the number of chemical analyses needed for the *ab initio* calculation of urinary supersaturation, Marshall and Robertson have empirically analyzed the results of their *ab initio* calculations of urinary supersaturation and have devised nomograms for estimating supersaturation with considerably fewer chemical analyses [10]. Only the chemical determination of citrate and oxalate pose a problem in practice. The nomogram approach obviates the citrate determination and access to a computer.

Semi-empirical method of Pak and Chu. In the method of Pak and Chu [5], the concentration of dissolved stone salt is measured before and after equilibration with solid stone salt. Relative supersaturation, A_i/A_o, for whewellite is calculated with

$$A_i/A_o = [TCa_i][(TC_2O_{4,i})[(f_i)^8[TCa_0][TC_2O_4)_0](f_0)^8. \quad (9)$$

Pak and Chu have devised an approximation to estimate f_i and f_o. Detailed calculations, however, show that f_i differs from f_o by <0.001; thus, as noted, $f_i \approx f_o$ and can be ignored because they cancel in Equation 9. The major innovations in the Pak and Chu method are the disregard of the complexing of the precipitating ions that occurs with calcium, phosphate, and oxalate in urine and urine-like solutions and the use of total concentrations, instead of ion concentrations, in calculating A_i/A_o with Equation 9. An examination of four calculations on urine, randomly selected from our archives of calculations, showed that the average A_i/A_o for whewellite calculated by Equation 9 is 2.4 ± 1.2% greater than that generated by the *ab initio* calculation. This small error is expected in estimates of A_i/A_o resulting from the use of Pak and Chu's approximations and is quite acceptable.

The preceding theoretical comments made about the semi-empirical estimation of A_i/A_o for whewellite also apply to Pak and Chu's method for determining brushite A_i/A_o. It is worth noting, however, that the trouble Pak and Chu take in calculating $[HPO_4^{2-}]$ from total phosphate concentration and pH can be neglected. Under their assumptions, Equations 4 and 5b require that $[HPO_4^{2-}] = [\alpha TPO_4]$. If the pH is constant, α is constant and will cancel out when Equation 9 is used for calculating A_i/A_o; see Equation 9 and replace $[TC_2O_4]$ with $[HPO_4^{2-}]$. If $pH_i \neq pH_o$ then α is not constant; but the semi-empirical method is then not valid for phosphate precipitations. The correspondence between *ab initio* and semi-empirical estimates of brushite A_i/A_o is good [11]. Parenthetically, although the calculation is trivial, *ab initio* estimates of A_i/A_o for uric acid agree well with semi-empirical estimates by Pak et al [12].

The fundamental conceptual problem in comparing the *ab initio* calculation and the semi-empirical equilibration method is that the former does not calculate A_o but rather uses a thermodynamic A_o that has been extensively characterized in simple aqueous solutions. The semi-empirical equilibration technique uses an A_o developed by experimental observation on urine. *Ab initio* calculated (A_i/A_o)'s for calcium oxalate in urine are two to three times greater than the (A_i/A_o)'s generated by the Pak et al method [11], a distressing disparity. I hasten to point out the *ab initio* calculation appears to be capable of calculating A_i. Robertson has shown good correspondence between calculated and measured $[Ca^{2+}]$ in urine [4]. And we have been able, in my laboratory, to predict, to within 20%, the experimentally measured A_o in artificial urine that contains no crystal-growth inhibitors, such as pyrophosphate and macromolecules. *Ab initio* calculations have a proven record of utility in other systems.

One possible explanation of the differing results produced by the two methods with urine is that they use different estimates of A_o. This line of reasoning requires that the thermodynamic A_o be less than the A_o empirically measured in urine. It may be speculated that the empirically measured A_o is larger than the thermodynamic A_o because of crystal-growth in-

hibitors in urine. This speculation, which remains untested, arises from observations that crystals covered with a film of inhibitor will not continue to grow when $A_c > A_i > A_o$, in which A_c is a critical concentration and by empirical testing would appear to be A_o [13]. Ohata and Pak [14] have shown that ethane-1-hydroxyl-1,2-diphosphonate, a crystal-growth, inhibitor, gives an apparent A_o greater than the thermodynamic A_o with brushite. In support of this concept, there is some evidence that the use of a large excess of the solid salt yields an empirically derived A_o that closely approximates the thermodynamic A_o [15]. Another possible explanation of the difference between the *ab initio* and semi-empirical estimates of whewellite supersaturation in urine is that unappreciated urinary chelators of oxalate, such as spermine, may be present in sufficient concentration to invalidate the *ab initio* calculations. A third possible explanation for the difference is that true equilibrium was not obtained in the semi-empirical method. A critical evaluation of the approach to equilibrium with the semi-empirical method has not yet been published.

Semi-empirical method of Gill, Silvert, and Roma [6]. The method of Gill et al has been applied thus far only to whewellite A_i/A_o estimation. The method differs from Pak and Chu's method [5] in that an oxalate tracer (^{14}C) is added to the system, and only changes in the oxalate concentration are measured. *Ab initio* calculations in my laboratory on four randomly selected urine samples showed that setting $[TCa_i] = [TCa_o]$ leads to an average error of $3.7 \pm 2.0\%$ in estimating A_i/A_o with equation 9, which is acceptable.

The primary drawback to the Gill et al method is that solid-state diffusion of ^{14}C-oxalate into the seed crystals of whewellite is appreciable and makes the method theoretically valid only at the limit of no seed crystals. That theoretical restriction is experimentally implemented by minimizing the amount of seed crystals; this in turn increases the system's relaxation time and thereby increases uncertainty about the experimental estimate of A_o. In a study of 23 urine samples that correlated equilibrium calculations of A_i/A_o with estimates by the Gill et al method, the correlation coefficient was 0.86 [16]. The apparent problem of estimating A_o for $CaC_2O_4 \cdot H_2O$ that is intrinsic in the Pak and Chu method also applies to the Gill method.

A comment on the usefulness of A_i/A_o. The estimation of A_i/A_o, by whatever method, is clinically useful. Such estimations are an extension of the same reasoning that prompts measurement of 24-hr urinary calcium by those who do not comprehend the pervasive nature of the second law of thermodynamics. Estimates of A_i/A_o, used in cluster analysis in conjunction with estimates of urinary-aggregation inhibitor concentrations, have been used to distinguish stone-formers from non-stone-formers [8]. Because crystal-growth inhibitor activity is often correlated with aggregation inhibition, the successful use of aggregation inhibition in the cluster analysis may be due to the inhibitor altering A_o instead of a direct effect on aggregation. Further experimental work is needed to resolve the true significance of aggregation inhibitor in the analysis of clustering with A_i/A_o estimates.

The potential efficacy of antistone therapy has been evaluated by A_i/A_o estimates [17, 18]. In the case of calcium oxalate, the semi-empirical method is probably more valid, and its use is recommended until a better concordance can be made between calculated and measured A_i/A_o.

It has been experimentally established that stone-formers' urine is supersaturated with the salt of the stone that they are growing [9, 19]. The conceptual problem is that some non-stone-formers' urine at times seems to be just as supersaturated as urine from stone-formers, but they fail to form stones. The difference must lie in the boundary conditions, the stochastic nature of the process, or urinary inhibitors of nucleation, crystal growth or aggregation, or some as yet undiscovered principle.

Nucleation

Nucleation is the initial event in a phase transformation (e.g., stone-salt precipitation). Except near the spinodal (defined below) where kinetic considerations may take precedence, the onset of nucleation is governed by the energy given up in forming a new-phase volume (ΔG_v) and by the energy required to form the surface of the new phase [1, 20]. If the new surface is well-defined in space, the situation is classical, and the associated surface energy is the familiar liquid-solid interfacial tension (σ). If the surface of the nucleus is diffuse, however, the situation is nonclassical and the surface energy is related to the energy required to form a gradient between the bulk of the two phases [21]. A relatively recent and readable exposition of the physical chemistry of nucleation in liquids and solution has been written by Walton [22]. The following brief discussion of nucleation develops points of view that have been neglected in the literature on urolithiasis, but that can and should be experimentally pursued in current stone research.

Classical homogeneous nucleation. As with most physicochemical processes, we start with free-energy considerations. The standard free-energy change (ΔG°) resulting from the formation of a spherical new phase can be written as

$$\Delta G^\circ = \frac{\pi l^3}{6}\Delta G_v + \pi l^2\sigma, \qquad (10)$$

in which l is the sphere diameter. If l is too small, the surface-energy term prevails, and the new phase will dissolve. If l is large enough, the volume-energy term prevails, and the new phase will either stay the same size or grow. The critical value of l (l^*), needed for a new particle to remain stable or grow, is given by

$$l^* = 4\sigma/\Delta G_v. \qquad (11)$$

In principle, σ can be calculated, but in practice, it is usually experimentally measured. However,

$$\Delta G_v = \frac{-mkT}{v}\ln(S), \qquad (12)$$

in which m is the number of ions in the neutral molecule, v is the molecular volume, k is the Boltzmann constant, T is absolute temperature, and A_i/A_o is denoted as S to simplify the notation (Fig. 2).

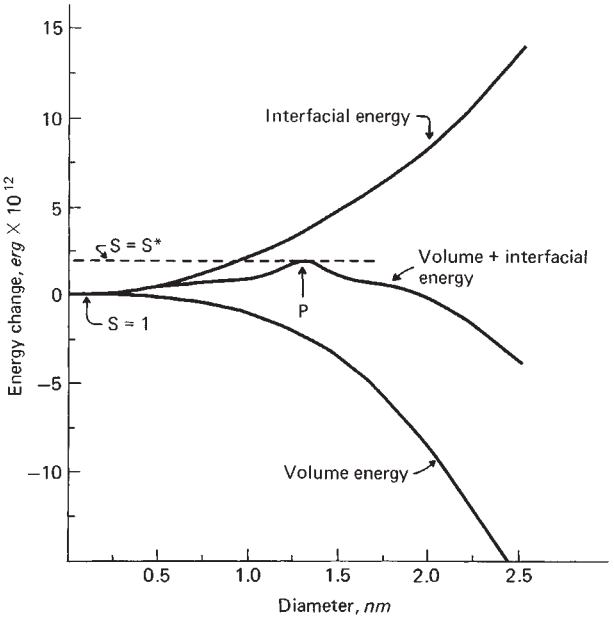

Fig. 2. *Calculated energy changes in the formation of a homogeneous nucleus of calcium oxalate.* Energy change was calculated with Equation 10. ΔG_v was calculated with Equation 11. The critical radius (l^*) was 1.3 nm, surface energy (σ) was 67 erg/cm^2 [20]. The point P is l^*. The energy change associated with point P is equivalent to the energy required to laterally displace the center of mass C′ in Fig. 1 to be over the pivot point. Past point P, increasing the nucleus diameter causes a negative energy change, and hence, continued growth of the nucleus is spontaneous.

If G^* is ΔG°, evaluated at $\partial\Delta G^\circ/\partial l = 0$, then the Equation 11,

$$\Delta G^* = \frac{-16\Pi\sigma^3\nu^2}{3(mkT\cdot \ln S^*)^2} \qquad (13)$$

$$= \phi\sigma^3/(\ln S^*)^2 \qquad (14)$$

with ϕ defined by Equation 13. Because ΔG^* is equivalent to an activation energy, the rate of nucleation (J) is written as

$$J = F\exp(-\Delta G^*/kT), \qquad (15)$$

$$\text{or} \quad J = F\exp(\phi\sigma^3/kT(\ln S^*)^2). \qquad (16)$$

The value of F is not known with certainty, but is usually taken to be 10^{25} to 10^{32}.

S^*, the metastable limit, can be experimentally measured in two ways. In the first, J is measured as a function of S. Because it is virtually impossible to prepare solutions that are free of particulate matter that acts as sites of heterogeneous nucleation at $S < S^*$, J increases perceptibly with S; but in the region of S^*, dJ/dS abruptly changes from ~0 to a large positive value. The position of the discontinuity of dJ/dS on the S axis is an estimate of S^*. Alternatively, the mean particle size resulting from a burst of precipitation increases as S increases and goes through a maximum at S^*. By measuring S^* and J, the values of σ, ΔG^*, and l^* can be calculated from Equations 11, 14, and 16, respectively. It is in this fashion that many of the estimates of σ used in discussing nucleation theory have been obtained. This experimental approach has been used with calcium oxalate. It was found that $S^* = 31$, $\sigma = 67$ erg/cm^2, and $l = 1.3$ nm [20]. Other stone salts have not been studied in this manner.

Classical heterogeneous nucleation. Heterogeneous nucleation occurs when a foreign surface reduces the metastable limit by catalyzing nucleation. Theories of heterogeneous nucleation usually start with the theory of homogeneous nucleation, outlined above, and proceed both to modify the activation free energy, ΔG^*, and increase the pre-exponential term by ~10^8 [20]. As discussed by Turnbull and Vonnegut [23], if the nucleus forming on a catalyzing surface is a sector of a sphere, then a contact angle (θ) can be defined, such that

$$\theta = \cos^{-1}\{(\sigma_{cl} - \sigma_{cn})/\sigma_{ln}\}, \qquad (17)$$

in which n refers to nucleus, c to catalyst, and l to liquid (Fig. 3). If ΔG^*_c is the catalyzed activation energy, then

$$\Delta G^*_c = \Delta G^* f(\theta), \qquad (18)$$

$$\text{with} \quad f(\theta) = (2 - \cos\theta)(1 - \cos\theta)^2/4. \qquad (19)$$

Equation 18 indicates that the free-energy barrier to

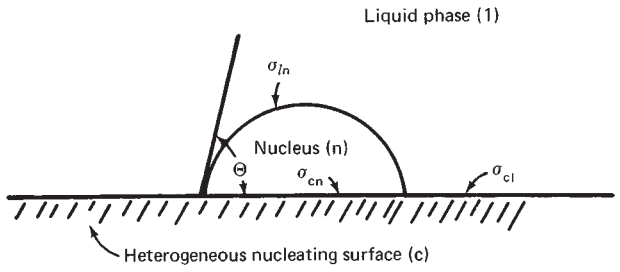

Fig. 3. *Schematic view of a drop heterogeneously nucleating at a liquid-solid interface.* The σ's indicate site of surface energy.

heterogeneous nucleation is reduced by a factor that is a function of the affinity of the nucleus for the catalytic surface.

It is well established that potent nucleation catalysts have crystal planes with lattices whose dimensions are similar to the dimensions of a low-index plane of the crystal that is being nucleated. Indeed, Lonsdale [24] caused considerable excitement in stone research when she published a list of low-index lattice dimensions for stone crystals. Many good matches were evident. However, because of the strain energy in a newly formed nucleus that results from a less-than-perfect lattice match, the goodness of a lattice match, by itself, is not a reliable predictor of the nucleation potency of a surface. Matching of crystal lattices and strain energy do not appear explicitly in Equation 18, so we will briefly consider how these physical constraints can be incorporated into nucleation equations. Consider a catalytic crystal plane with lattice parameter $(a)_c$ nucleating a crystal plane with lattice parameter $(a)_o$. The degree of mismatch (δ) is

$$\delta = ((a)_c - (a)_o)/(a)_o, \qquad (20)$$

and the resulting lattice parameter (x) for the strained nucleated crystal at the catalytic interface will be a compromise between $(a)_c$ and $(a)_o$. The strain (ϵ) in the new crystal is

$$\epsilon = |(x - (a)_o/(a)_o|, \qquad (21)$$

such that $\epsilon < \delta$. The actual disregistry (D) between the nucleated crystal and the catalytic surface is

$$D = \delta - \epsilon. \qquad (22)$$

With this construct, the surface energy for the interface between the nucleus and the catalyst is written as

$$\sigma_{cn} = \gamma + \alpha D, \qquad (23)$$

in which γ is an interaction term determined by physicochemical factors and αD is a structural term proportional to the crystal-lattice dislocation density in the developing nucleus. The heterogeneous-nucleation equation analogous to Equation 17 is

$$\cos\theta = \{\sigma_{cl} - \gamma - \alpha D\}\ \sigma_{ln}. \qquad (24)$$

It follows that the equation analogous to Equation 10 is

$$\Delta G = V(\Delta G_v + C\epsilon^2) + 2\Pi r^2(1 - \cos\theta)\sigma_{cl} + \Pi r^2(1 - \cos^2\theta)(\sigma_{cn} - \sigma_{ln}), \qquad (25)$$

in which V is the volume of the sector and $C\epsilon^2$ is the strain-energy density, with C expressed in terms of elastic coefficients of the newly forming crystal. Maximizing Equation 16 with respect to nuclear radius gives an equation analogous to Equation 14:

$$\Delta G^*_c = 4\Pi(\sigma_{cl})^3(2 + \cos\theta)(1 - \cos\theta)^2/3(\Delta G_v + C\epsilon^2)^2. \qquad (26)$$

Eliminating ϵ from Equation 26 gives

$$\Delta G^*_c = \Pi\alpha^2\sigma_{cl}\,\delta^2(1 - |\Delta G|/C\delta^2)/\{\Delta G_v + C\delta^2(1 - (1 - |\Delta G_v|/C\delta^2)^{1/2})\}. \qquad (27)$$

The nucleation potency (P) of a catalyst is proportional to $1/(\beta\sigma_{cl} - \alpha\delta)$, with $\beta = 1 - (\sigma_{ln} - \gamma)/\sigma_{cl}$. The validity of Equation 27 in predicting the efficiency of heterogeneous-nucleation catalysis in stone-salt precipitation has not been tested experimentally. In practice, it is thought that δ usually needs to be less than 0.1 for P to be large, although one case of good catalysis of nucleation with $\delta \sim 0.5$ has been reported [23]. It is noteworthy that many instances of $\delta < 0.1$ can be found in the list of stone-salt lattice parameters provided by Lonsdale [24].

Classical coherent (epitaxial) vs. noncoherent nucleation. When δ is small, nucleation is said to be coherent. When δ is large, but the surface has high catalytic potency because β is large, nucleation is noncoherent. "Epitaxial nucleation" has been commonly used recently in discussions of precipitation in biologic systems. There is growing support, however, for the belief that epitaxial nucleation occurs on surface defects that have catalytic potency, and once the nucleus is established, it migrates to the bulk surface, where it may proceed with oriented (epitaxial) overgrowth [22, 25].

Other models of nucleation have been proposed, of which many are variations of the nucleation schemes that have been discussed here. A major exception to this generalization is the formulation of Nielsen [1], who treats nucleation rate as a chemical reaction and uses his experimental observations (light-scattering) to compute reaction orders, many of which are nonintegral.

Nonclassical nucleation: a) Spinodal decomposition. Many urinary stones and crystallurias contain

numerous spherulitic particles [26]. Spherulitic growth is not predicted by classical-nucleation equations. One theory that has been advanced to explain the spherulitic growth holds that because spherulitic growth systems are multicomponent systems, have small coefficients of self-diffusion, and crystallize slowly, plane crystal faces in these systems suffer instabilities of profile, which give rise to noncoherent bundles of fibers. The fiber width is the ratio of the self-diffusion coefficient to the crystal growth rate [27].

Another approach to spherulitic growth is that of Cahn and Hilliard (discussed by Uhlmann and Chalmers [28]), who have taken a very general approach to nucleation in solid solution and formulated the nucleation free-energy change in a system, ΔG_{syst}, as

$$\Delta G_{syst} = \int_v [g(S) + K(\nabla S)^2] dv, \qquad (28)$$

in which S is relative supersaturation.

Equation 28 is seen to be analogous to Equation 10, in that g(S) is equivalent to ΔG_v. Actually, g(S) is the average ΔG_v for the system. $K(\nabla S)^2$ is equivalent to the surface-energy term in Equation 10. The "surface energy," however, is proportional to the square of the concentration gradient.

Following the suggestion by Sears [21], we now observe how Equation 28 can be used to make some qualitative statements about nucleation. A plot of G_{syst} versus S shows a point of inflection at $\partial^2 G_{syst}/\partial S^2 = 0$. The locus of points ($S_s$) at various temperatures at which the second derivative of G with respect to S equals zero is called the "spinodal." When $S < S_s$, the system is stable with regard to low-amplitude thermal fluctuations in concentration; i.e., if a large concentration gradient does not occur, then precipitation will not occur. This is the classical situation. However, if $S > S_s$, then the system is liable to undergo precipitation in the presence of low-amplitude thermal fluctuations in concentration. This is the nonclassical case. Another qualitative distinction demarcated by the spinodal is that as the nucleating supersaturation increases, when $S < S_s$ the radius (r) of the resulting nucleus decreases, whereas when $S > S_s$, the radius of the resulting nucleus increases with nucleating concentration. The increase in radius is due chiefly to the formation of a thick diffuse nuclear boundary. Recall that, for the classical case, Equation 11 states that $\Delta G_v^* = 2\delta/r^*$. Equation 11 imposes a relationship between ΔG_v^* and r^* that must be obeyed, if there is to be classical nucleation. That is, as ΔG_v^* becomes large, r^* becomes small, and *vice versa*. Because Equation 12 says that $\Delta G_v^* = (mkT \cdot \ln S^*)/v$, r^* becomes small as S^* becomes large. Consider, however, the radius of a nucleus to be composed of two parts: a central part with radius r_0 and a diffuse boundary part τ_0, so that $r^* = r_0 + \tau_0$. Thus, as τ increases in size, the gradient of S between the solution and the r_0 part of the nucleus becomes smaller. ΔG_{syst} in Equation 28 can, therefore, be made smaller at large supersaturations by building a nonclassical large nucleus with a diffuse boundary that has a small concentration gradient. Combining Equations 11 and 12 gives

$$S^* = \exp(2\delta v/(mkTr^*)). \qquad (29)$$

Equation 29 says that, for a given nuclear radius, if the experimentally measured S is greater than predicted, the situation is no longer classical. Alternatively, at supersaturations greater than S^*, Equation 29 predicts a nonclassical nucleus, inasmuch as the radius will be bigger than r^*. When the nucleus becomes larger than the classical size, part of its size consists of its diffuse boundary. The thicker the boundary, the smaller the gradient, ∇S, and the gradient energy. Therefore, as S becomes large, it becomes energetically economical to form a nucleus that is nonclassical. The nonclassical nucleus has a disordered interior; it can be spherulitic, polymicrocrystalline, or glassy [21]. Nonclassical nucleation of the type under discussion (spinodal decomposition), is commonly seen in metals and polymer solutions. Indeed, it is said that because of the relatively large lattice units of polymer crystals, it is difficult to obtain the classical type of nucleation in polymer solutions. A direct demonstration of spinodal decomposition in aqueous electrolyte solutions has not been made. Garten and Head [29], however, concluded from a study of crystalloluminescence that soluble and poorly soluble salts first precipitate as glassy objects that undergo a solid-state phase transformation to crystallinity. They were able to observe the transformation because crystalloluminescence can be electronically detected. Crystalloluminescence is a phenomenon that is consistent with a spinodal decomposition type of nucleation.

Nonclassical nucleation: b) Secondary nucleation. Chemical engineers have recognized that when a crystal surface is contacted by a solid object, such as another crystal, one or more nuclei can be produced. The production of nuclei is directly related to the energy of the contact. This is a significant consideration in a commercial crystallization process. In urine, however, where the concentration of crystals is around 10^4/ml or less [30], it is likely that secondary nucleation plays a small role. For example, when 2-μm whewellite particles impact at a relative velocity

of 10 mph (447 cm/sec), the kinetic energy of the contact is less than 10^{-5} erg, which should yield less than 10^{-9} nuclei per contact if the contact area is 1-μm^2 [31]. Collision theory predicts that if there are 10^4 particles/ml with 20-μm diameters, randomly moving at 5 mph, there should be less than 2×10^{-3} collision/(ml·sec) [32]. Therefore, it is expected that fewer than 300 secondary nucleations occur each day–less than one ten-thousandth of the nucleation activity occurring in urine when 10^7 particles/day are being passed. With this analysis, it is expected that the secondary-nucleation rate would vary with the square of the number of particles. If the primary-nucleation rate increases by a factor of 10^3, the ratio of secondary to primary nucleation approaches unity.

Current knowledge about nucleation of stone salts and its relevance to urolithiasis. Unless extraordinary precautions are made, most clean solutions contain 10^6 to 10^8 submicroscopic particles per milliliter [20]. Many of these particles have high catalytic potency for nucleating precipitation of a variety of salts, including stone salts. Therefore, it is customary not to expect homogeneous nucleation in a precipitation system, unless the concentration of precipitated particles is greater than 10^6/ml.

Robertson [30] has reported that crystal particle counts in urine of stone-formers are about 10^4/ml, compared with the 10^6 criterion that has been suggested for homogeneous nucleation [22]. As pointed out by Trump, Dees, and Kim, urine is rich in cellular debris that probably can catalyze nucleation [33]. Therefore, it should be tentatively concluded that most, if not all, stone-salt nucleations in urine are heterogeneous or nonclassical, or both.

Malek and Boyce have hypothesized that crystalline urinary-stone nuclei are manufactured in renal tubular cells and are extruded into urine [34]. There is no information on the formation of these hypothesized nuclei. But for the purpose of this discussion, the process suggested by Malek and Boyce [34] can be considered another case of either nonclassical or heterogeneous nucleation.

Nielsen [35] has shown that in filtered solutions of poorly soluble salts, the induction time for precipitation (τ) obeys

$$\tau = gC^n, \qquad (30)$$

in which C is the square root of the molar ion concentration product of the precipitating salt and g and n are empirical constants. For calcium oxalate at 25°C, $g = 1.03 \times 10^{-7}$ sec, and $n = -3.33$. According to this, the lower limit for the induction period for concentrated urine ($C = 1.70 \times 10^{-3}$ M) is ~2.9 min, which is well within the transit time across the kidney. Even though the solutions that Nielsen used were filtered, we must assume in this case, in the absence of evidence to the contrary, that the nucleation was heterogeneous, which is also probably the case in urine.

Robertson, Peacock, and Nordin have measured the S that gives a perceptible precipitation in 15 min at 25°C for various stone salts [19]. No serious attempt to determine whether these precipitations resulted from homogeneous or heterogeneous nucleation has been reported, so one must conclude that the set of "critical" supersaturations reported by Robertson and his coworkers is for heterogeneous nucleation.

In the case of struvite, uric acid, and cystine, published estimates of S* provide a useful criterion for separating stone-formers from non-stone-formers. Robertson's estimates of S*, however, do not provide a reliable criterion for distinguishing formers from non-formers of calcium oxalate and sterile calcium phosphate stones. One possible explanation being advanced for this failure is that the urine of stone-formers contains more heterogeneous nucleating particles than that of non-stone-formers [36]. A few workers [36–39] have investigated Lonsdale's suggestion [24] that various stone salts could act as coherent heterogeneous nucleation catalysts for other stone salts. These workers have shown that given sufficient supersaturation and appropriate pH, brushite, hydroxyapatite, whewellite, and monosodium urate will nucleate each other. Inasmuch as the maximal supersaturation relief in 30 min in the systems that were studied was 20% or less, it is not clear how relevant these observations are to the biologic problem of urolithiasis. Transit time across a kidney is < 10 min (i.e., volume/flow rate). With data presented by Pak, Hayashi, and Arnold [37], one can calculate that a 20% solution depletion in 30 min implies a linear growth rate of less than 1.6 nm/min, if all the particles in the test system are growing at the same rate. To make this calculation, we use the relation

$$\left(\frac{l_2}{l_1}\right)^3 = \left(\frac{m_2}{m_1}\right), \qquad (31)$$

in which l is a characteristic length and m is a mass of particles. The densities of stone particles are all ~2, so it is not necessary to calculate rim growth. Furthermore, we have assumed that the average particle size is 10 nm; a smaller particle would imply a lower growth rate. In view of the transit times, a worst-case growth rate of 1.6 nm/min does not constitute a serious health hazard. If only a few particles nucleate

in the *in vitro* heterogeneous nucleation systems, however, then the implied growth rate would be far greater, perhaps even significant. Particle size distribution in these systems was not analyzed, so the biologic significance of *in vitro* heterogeneous nucleation with respect to urinary stone salts would recognize that total growth is the convolution of nucleation and growth. Given the experimental observation of solution depletion and a valid growth-rate law, the nucleation rate can be readily separated from the growth rate with Laplace transforms [40]. The data published thus far do not merit such a detailed analysis.

Particle growth

The detailed growth history of a urinary stone is unknown. From an investigative point of view, perhaps the most informative studies have been on the rate of particle growth of precipitates in urine. If the product of particle growth rate and particle transit time is small, relative to the diameter of lumen through which the growing particle must pass, then the particle will be passed harmlessly and will not develop into a macroscopic stone. In particle-growth studies, a distinction must be made between crystal growth and growth by aggregation. A slurry of crystals in a supersaturated solution will increase in size and under appropriate conditions will aggregate, in which case the particle size distribution is not the same as the crystal size distribution. Urinary stones are typically polycrystalline masses [26], and the particle size distribution in urinary stones is not identical with the crystal size distribution. Even the crystalluric particles from a stone-former are polycrystalline [41], and it follows that the crystalluric particle size distribution does not equal the crystal size distribution. It is necessary to understand the kinetics of the particle size distributions that occur in urine if we are to understand how urinary stones form. We are just beginning to develop an understanding of urinary stone crystal growth and aggregation mechanisms. What little work is being done usually does not distinguish between the two mechanisms. There are at least five methods for studying crystal growth, as described below.

Single crystals. Single-crystal studies have the advantage that aggregation is not a problem; therefore, growth measurements can be made on individual faces. However, single-crystal studies have not been done yet on stone crystals.

Spontaneous precipitation. In spontaneous-precipitation studies, an unstable supersaturated solution is allowed to precipitate spontaneously. To distinguish between crystal growth and aggregation, it is necessary to use two independent monitoring methods. It is convenient to observe the early part of the reaction by measuring solution depletion with electric conductivity and by measuring particle size distribution with light-scattering. As the reaction goes toward completion, wet chemical methods of measuring solution depletion and Coulter counter methods of particle size distribution analysis are often more convenient. Doremus, Gardner, and McKay [42] have used spontaneous precipitation to study growth of stone-salt particles. They observed that the order of the growth reaction for calcium oxalate is 3 when $A_i/A_0 \geqslant 5$. They noted that other workers had observed that the order of the reaction at lower supersaturations is 2 [43]. The growth equation Doremus et al used to analyze their data is

$$(dW/dt) = kb(1 - W)^n, \qquad (32)$$

in which k is a growth constant, b is a system parameter, W is the extent of reaction, and n is the order of the reaction [42]. One potential problem with Equation 32 is that it does not explicitly account for change in particle surface area, which in the spontaneous precipitation, undergoes considerable change in the early part of the reaction. In this case, one might expect the equation of Johnson and O'Rourke [44] to be more appropriate:

$$(dW/dt) = kb^q(1 - W)^n, \qquad (33)$$

in which b is now a function of W, and q is an empirical constant that is usually $\frac{2}{3}$. This equation, by accounting for changing surface area, might provide a concordance between high- and low-supersaturation growth-rate reaction orders. Nielsen [35] reported that calcium oxalate in spontaneous precipitation does follow Equation 33, but could not decide whether n was 3 or 4. In their study of spontaneous precipitation of calcium oxalate, Doremus, Gardner, and McKay reported that the initial precipitate is $CaC_2O_4 \cdot 3H_2O$, which undergoes solid-state transformation with an activation energy of 45 kcal/mole (relaxation time, ~4 hr at 37°C) [42]. Voided calcium oxalate particles ordinarily are $CaC_2O_4 \cdot H_2O$ (whewellite) or $CaC_2O_4 \cdot 2H_2O$ (weddellite). It is of considerable interest to know what the crystal is when urine is leaving the renal papillae during calcium oxalate crystalluria. It is hoped that such information will soon be available.

Füredi-Milhofer et al [45] have observed that burst precipitations of brushite also follow Equation 33, with $q = \frac{2}{3}$ and $n = 2$, except that in this case the independent variable W was the reacting ion concentration product.

The concept of a formation product and spontaneous precipitation. This section digresses from the discussion of crystal growth mechanisms in order to comment about the use of spontaneous precipitation in studying formation products. A formation product is the minimum ion activity product needed to induce a salt to precipitate. It should be clear from the preceding discussion that a formation product is an expression of a metastable limit. Some investigators have attempted to estimate the formation product by observing the minimum concentration or ion activity product needed to cause a spontaneous precipitation within some arbitrarily fixed time interval. The method of detecting onset of precipitation is also arbitrary, inasmuch as some detection methods are more sensitive than others. Before I attempt to draw inferences about experimental measurements of the formation product, it is instructive to look at some experimental results. In my laboratory, we have investigated the effect of allopurinol on calcium oxalate precipitation by using a Coulter counter to measure the number *(N)* and the average size of particles created by a spontaneous precipitation of calcium oxalate at various initial supersaturations. As predicted in the section on classical homogeneous nucleation, a plot of N vs. supersaturation (Fig. 4) shows a sudden upswing and suggests a calcium oxalate metastable limit for homogeneous nucleation of $S > 100$. Also, as predicted, a plot of the average particle diameter vs. relative supersaturation (Fig. 5) goes through a maximum located between a relative supersaturation of 80 and 100, which suggests that the metastable limit for homogeneous nucleation is $\geqslant 80$. Previous estimates in the urolithiasis literature of the metastable limit for homogeneous nucleation of calcium oxalate have never exceeded a relative supersaturation of 11 [19]. Using an approach like the one outlined for Figure 5, Walton [20] reported that the homogeneous nucleation metastable limit for calcium oxalate at 25°C is a relative supersaturation of 30.

Inasmuch as Figures 4 and 5 indicate that particles are nucleating at initial supersaturations less than the metastable limit, heterogeneous nucleation also occurs in the systems described by Figures 4 and 5. The information presented in the section on classical nucleation suggests that when both homogeneous and heterogeneous processes occur, the rate of nuclei formation (J_B) should be written

$$J_B = \sum_{i=1}^{n} F_i \exp(-\phi(f(\theta)_i \sigma^3 Z)) \qquad (34)$$

where $Z = (\ln S)^{-2}$, $i = 1$ is the homogeneous case in

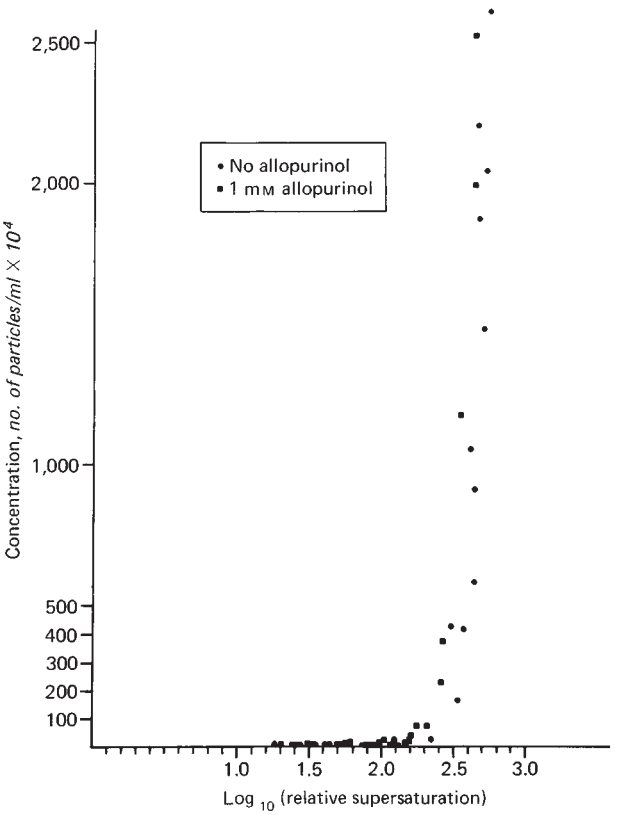

Fig. 4. *A plot of final numbers of calcium oxalate particles per ml resulting from a burst of precipitation vs. $\log_{10}$ (initial relative supersaturation).* The number of particles is taken to be the number of nucleation events (pH, 6.5; temperature, 38°C).

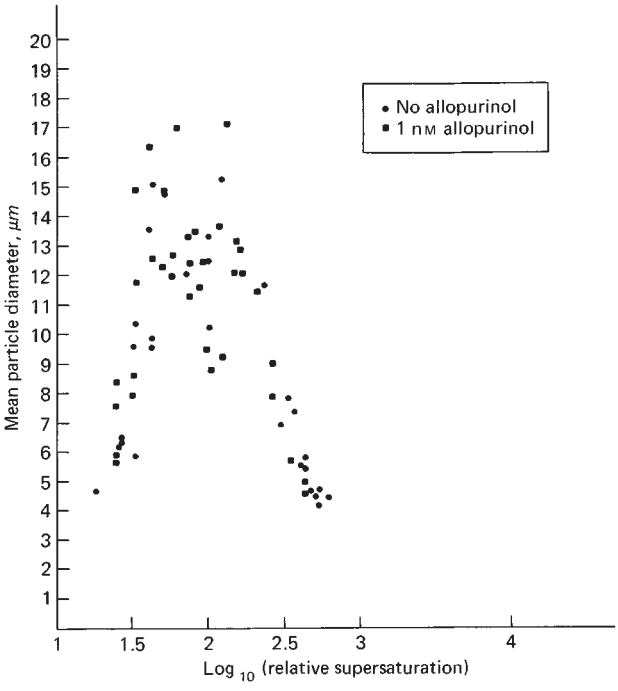

Fig. 5. *A plot of mean particle diameter vs. $\log_{10}$ (initial relative supersaturation).* Conditions are the same as in Figure 4.

which $f(\theta)_1 = 1$, and all the other $n - 1$ cases are heterogeneous nucleations with $(1 - f(\theta)_i)$ indicating the catalytic efficiency of the i^{th} class of heterogeneous nucleating site. The relation between Equation 34 and the Coulter counter measurements in Figure 4 is

$$N = \int_0^\infty J_B dt. \qquad (35)$$

The difficulty with integrating Equation 35 is that Z in Equation 34 is not available in analytic form. If, however, $(d^2Z/dt^2) \approx 0$ until $1 >> \exp(-\phi(f(\theta)_i\sigma^3 Z))$, then

$$N = \int_0^\infty \sum_{i=1}^{n} F_i \exp(-\phi(f(\theta)_i\sigma^3 Z))dt, \qquad (36)$$

and $$N = \sum_{i=1}^{n} Q_i \exp(-\phi(f(\theta)_i\sigma^3 Z(t = 0))) \qquad (37)$$

with $Q_i = F_i/(+\phi\sigma^3(dZ/dt)f(\theta)_i)$ and $(dQ_i/dt) \approx 0$.

A transformation of the data in Figure 4 to a plot of $\ln(N)$ vs. $Z(t = 0)$ shown in Figure 6 strongly suggests that the assumptions giving rise to Equation 37 are valid and that $n = 2$ (i.e., the experimental system has only one class of heterogeneous nuclei). Much of the information suggested by Figure 6 can be given intuitively simple interpretations. For example, since $f(\theta)_1 = 1$, the slope of the steepest limb of the curve is $-\phi\sigma^3$. ϕ is a combination of known physical constants; and we calculate, from Figure 6, that σ for calcium oxalate is 69 erg/cm^2, which is in excellent agreement with the reported value of 67 erg/cm^2 [20]. Since the slope of the other limb of the curve in Figure 6 is $-\phi\sigma^3 f(\theta)_2$, and $-\phi\sigma^3$ is known, $f(\theta)_2$ can be estimated. Furthermore, the intercept of the lower limb at $Z = 0$ is a count of the number of heterogeneous nuclei.

The important points to be gained from Figures 4, 5, and especially 6 are: *1)* Homogeneous nucleation of calcium oxalate in urine is most improbable. The kidney is incapable of creating sufficient supersaturation. It also follows that current methods of estimating apparent formation products measure either the catalytic efficiency of heterogeneous nuclei or an alteration in the liquid-solid interfacial energy of precipitating salts. *2)* The catalytic efficiency $(1 - f(\theta)_i)$ of heterogeneous nuclei in urine is experimentally measurable. Nucleation inhibitors in urine can act by altering either the calcium oxalate liquid-solid interface (σ) or the catalytic efficiency of heterogeneous nuclei ($f(\theta)_i$). Appropriate use of Equation 36 would permit evaluation of both effects. *3)* The number of nuclei in urine can be measured. The point of view developed in this section is a means of removing the ambiguity associated with existing observations of formation products.

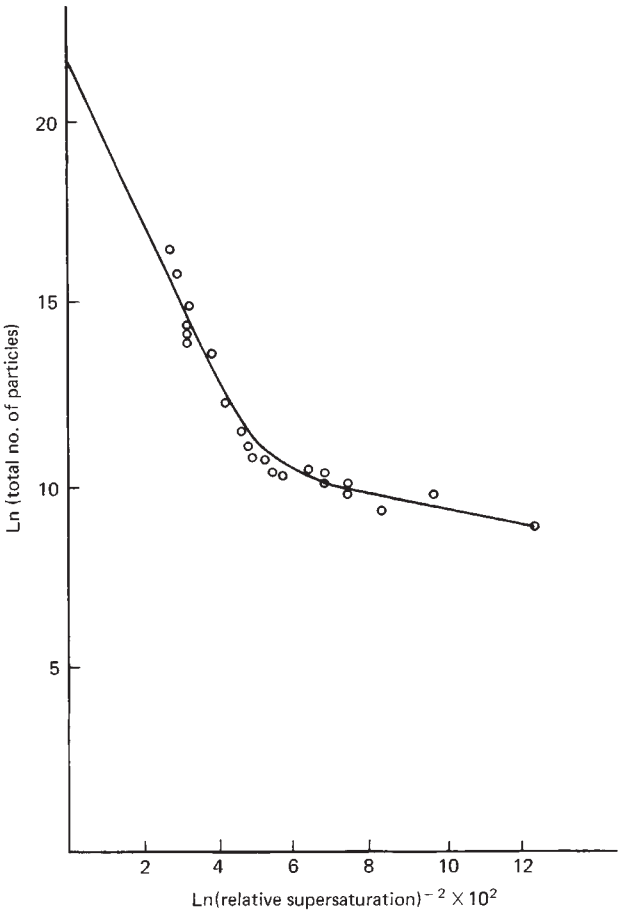

Fig. 6. *A transformation of data in Figure 4: The natural logarithm of the final particle concentration vs. (ln(relative supersaturation))$^{-2}$.* The presence or absence of allopurinol is suppressed. The *circles* are experimental data. The *solid line* is a least squares fit of Equation 37 with $n = 2$.

I hope that the preceding discussion and Figures 4–6 make it apparent that the concept of a unique formation product does not naturally derive from a theoretical foundation. A criterion for selecting a formation product is arbitrarily imposed by workers to provide a practical means of comparing the tendency to precipitate spontaneously in various urine samples.

Seeded crystals. To study seeded-crystal growth, seed crystals are added to a supersaturated solution, and the reaction is monitored. Nancollas and Gardner [43] and Marshall and Nancollas [46] have exploited the seeded-crystal growth system for whewellite and brushite. By experimental design, the surface-area change in the whewellite system was

small, and, using Equation 32, they observed that n = 2. However, in the analysis of the brushite experiments, the reaction variable, W, in Equation 32 was the reacting ion concentration product. Again, it was found that n = 2. In seeded crystal growth experiments, Meyer and Smith [47] measured the linear-growth-rate constant for whewellite with Equation 32 and with n = 2 at ~0.2 μm/min at urine concentrations of calcium and oxalate. (The method for transposing the rate constants in Equations 32 and 33 is presented elsewhere [48].) Because of growth inhibitors in urine, the growth rate is expected to be much smaller in urine than the value found in uninhibited simple solutions.

In our laboratory, working with seeded whewellite crystals, we have been unable to fit our data to Equation 32 with the reaction variable W being activity or concentration of either reactant, in contrast with the experience of Meyer and Smith [47] and Nancollas and Gardner [43]. Our systems, however, examine a larger range of supersaturation, a larger surface-area variation, and a larger extent of reaction than those of the other workers. We found that if A_i/A_0 is the reaction variable in Equation 32, good fits are obtained (Fig. 7), but the calculated surface-normalized rate constants have ratios approximating the ratios of the initial reacting surface. Therefore, it appears that an equation like Equation 33 should be used in the analysis. Because of the difficulty in integrating Equation 33, workers have used the differential form of the equation or tables of numerically integrated values. If a linear approximation is made of the $b^{2/3}$ term in Equation 33, the error is <5% if the final crystal weight is not greater than twice the initial crystal weight. This approximation is done as follows: with $S = A_i/A_0$, we write

$$dS/dt = -Ks(S - 1)^2, \qquad (38)$$

with K the growth-rate constant and s the surface area. Equation 38 is readily transformed into Equation 33. Note that with uniform growth,

$$s = s_I \left(\frac{M}{M_I}\right)^{2/3}, \qquad (39)$$

in which the subscript I indicates the initial value, and M is crystal mass. We note further that

$$M/M_I = 1 + (\Delta M/M_I). \qquad (40)$$

ΔM is approximated by

$$\Delta M \sim Q(S_I - S). \qquad (41)$$

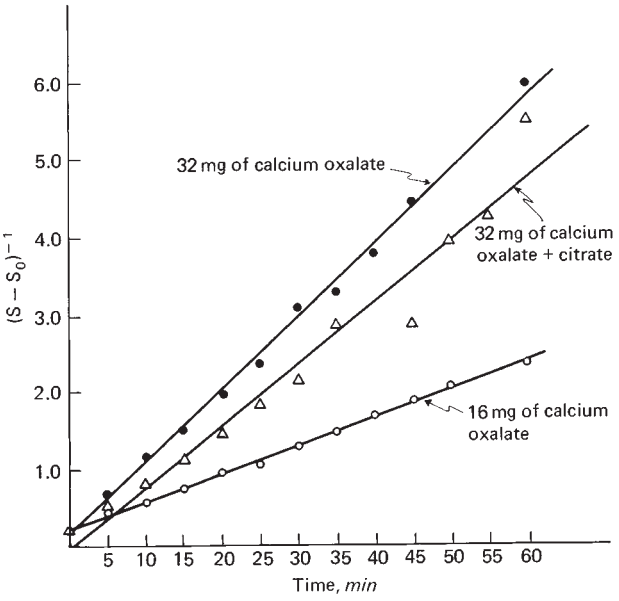

Fig. 7. *Seeded crystal growth rate data plotted in the integral form of Equation 32 with n = 2. Solid lines* are least squares fits. Either 16 or 32 mg of calcium oxalate seed crystals were used. The total system citrate concentration, when added was 50 μM (temperature, 38°C; pH, 6.5; and stirring, 600 rpm).

With Q a constant of proportionality,

$$Q = \Delta M^*/(S_I - 1), \qquad (42)$$

with ΔM^* being the maximal possible increase in crystal weight. Therefore,

$$\left(\frac{M}{M_I}\right)^{2/3} = \left(1 + \left(\frac{\Delta M^*}{M_I}\right)\left(\frac{S_I - S}{S_I - 1}\right)\right)^{2/3}. \qquad (43)$$

A second linear approximation results in

$$\left(\frac{M}{M_I}\right)^{2/3} = 1 + \frac{2}{3}\left(\frac{\Delta M^*}{M_I}\right)\left(\frac{S_I - S}{S_I - 1}\right), \qquad (44)$$

$$= 1 + V(S_I - S), \qquad (45)$$

with V defined by Equation 44. We further simplify with

$$\left(\frac{M}{M_I}\right)^{2/3} = \theta - VS, \qquad (46)$$

with $\theta = 1 + VS_I$. Thus,

$$dS/dt = -Ks_I(\theta - VS)(S - 1)^2, \qquad (47)$$

which is readily transformed to

$$-Ks_I dt = \left[\left(\frac{V^2}{\Delta}\right)\frac{1}{\theta - VS} + \left(\frac{V}{\Delta}\right)\frac{S}{(S-1)^2} + \frac{\theta - 2V}{\Delta}\left(\frac{S}{(S-1)^2}\right)\right] dS, \qquad (48)$$

in which $\Delta = (V - \theta)^2$. Equation 48 is readily integrated to

$$-Ks_1t = \left[\frac{V^2}{\Delta}\left(\frac{-1}{V}\right)\ln(\theta - VS) + \frac{V}{\Delta}\left[\left(\frac{-1}{S-1}\right) + \ln(S-1)\right] + \frac{(\theta - 2V)}{\Delta}\left(\frac{-1}{S-1}\right)\right] + \text{constant},$$
$$= G(S) + \text{constant}. \quad (49)$$

A plot of G(S) against r for a seeded-growth experiment is shown in Figure 8. Plots of ΔS against ΔC are linear for both our experimental system and for four random urine samples that we checked by *ab initio* calculation. This validates the first approximation that was used (i.e., Equation 41) and substantiates the estimated maximal error. Thus, from Figure 10 it appears that we have a growth law valid over reasonable ranges of concentration and surface-area change in a convenient integrated form. Of course, Equation 49 requires additional experimental verification.

Seeded-crystal growth studies have been done with hydroxyapatite crystals [49]. Depending on the concentration, however, one or more phases other than hydroxyapatite can be growing simultaneously, and the growth curves, even in simple solutions, are complex and difficult to quantitatively analyze. Calcium phosphate precipitates adsorb a variety of inhibitors known to be present in urine, and the actual growth rate of calcium phosphate in urine is a matter of conjecture.

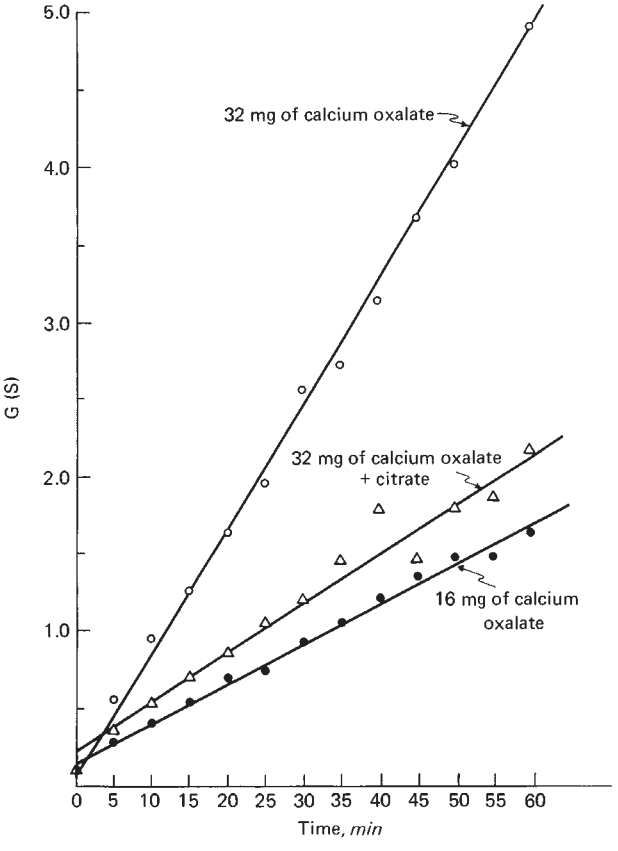

Fig. 8. *A plot of G(S) vs. time for seeded calcium oxalate crystal growth.* See text, Equation 49, for definition of G(S). Conditions are the same as in Figure 7.

Continuous crystallizers. A continuous crystallizer is a well-mixed compartment that continuously receives a supersaturated solution from an inlet and continuously or intermittently discharges its contents through an outlet. (The urinary tract can be considered as a series of continuous crystallizers, i.e., collecting duct, renal pelvis, and urinary bladder [50].) If the volume of the crystallizer and the concentration at the inlet are constant, the crystallizer dynamics are described by $n = n_0\exp(-x/ar)$, in which n is the concentration density of particles of size x, a is the growth rate, and r is the system volume divided by the flow rate [51]. Inasmuch as (an_0) is the nucleation rate, the system simultaneously gives information about crystal growth and nucleation rates. We have measured a whewellite growth rate of 0.79 μm/min with a calculated A_i/A_0 of 32. With a similar input, Miller, Randolph, and Drach observed that the growth rate of weddellite was less than 1 μm/min [52, 53].

The measurement of crystal growth rate in solutions has been dealt with at some length for several reasons. The most important is that the growth rate gives an upper bound on the time required to form a stone, and a firm grasp of growth rate permits us to start speculating about what is and what is not possible with regard to mechanisms in stone disease. In addition, with a clear understanding of how stone crystals grow, it will be possible to increase the sophistication of the *in vitro* tests done on urine to measure the tendency to grow stones and the effectiveness of antistone therapy.

Crystal growth in gels. Stone-salt crystals have been grown in gel systems [54, 55]. It is quite difficult to measure growth rate as a function of concentration in these systems because the analysis requires a complex diffusion calculation. However, growth in gel systems offers the best opportunity, so far, of growing large crystals (>100 μm in diameter) of stone salts. Gel systems typically yield crystals $\leq$1 mm.

Aggregation

Urinary stones and crystalluria particles are often described as polycrystalline aggregates. Robertson et al [8] are using aggregation inhibition as a factor in their evaluation of the stone-forming potential of

urine. Although it is generally agreed that aggregation is important in urolithiasis, very little work has been done on the details of stone-salt aggregation. The following is an outline of the problem as it pertains to urolithiasis.

When particles are about one centimeter in diameter or larger, gravitational forces tend to be greater than adhesional forces. But as the size of particles diminishes, the effect of adhesion relative to gravitation rapidly becomes dominant. For particles about one micrometer in diameter, adhesional forces are about a millions times greater than gravitational forces [56]. Thus, in dealing with fine-particle processes, adhesion must be taken into consideration. In dealing with crystalluria, it appears to be necessary to consider both particle-to-particle and particle-to-membrane adherence [48]. In addition, preliminary measurement of stone density has shown that stones have densities approaching the density of stone crystals [57]—very much higher than would be expected if stones formed purely by close-packed aggregation. Therefore, if aggregation is significant in urolithiasis, densification of the aggregate must also occur.

There are six basic mechanisms by which aggregates are held together [56]. In order of increasing energy, they are electrostatic attraction, van der Waal forces, liquid bridge, capillarity, viscous binder, and solid bridge. Because there is total immersion, liquid bridges and capillarity are not expected to play a large role in crystalluria particle interaction or in urolithiasis. Because of the zeta potential on particles immersed in urine, the electrostatic forces, if significant at all, will be repulsive. It is expected, on the basis of protein-adsorption isotherms [58], that each calcium oxalate particle in urine is coated 75% or more with a monomolecular layer of protein that may act as a viscous binder. Solid bridges can occur only after particle-to-particle apposition due to other adhesive forces. Therefore, we write in a qualitative way for particles in urine,

$$\text{force of adhesion} = \text{van der Waal} - \text{electrostatic} + \text{viscous binding} \quad (50)$$

For two spheres of equal size,

$$\text{van der Waal} = h\omega r/16\Pi a^2, \quad (51)$$

in which $h\omega$ is a tabulated function, r is the radius, and a is the separation distance;

$$\text{electrostatic} = \epsilon\epsilon_0 \Pi\psi^2 r/2a, \quad (52)$$

in which ϵ and ϵ_0 have their customary electrostatic meaning of electric permitivity, and ψ is the surface contact potential; and

$$\text{viscous binding} \geq M(\theta - RT\ln(k))h(a), \quad (53)$$

in which M is moles of binder, θ is the reference energy, R is the universal gas constant, T is the absolute temperature, k is the reciprocal of the concentration at which half surface saturation by the viscous binder occurs, and h(a) is a Heaviside unit function = 1 for a $\leq \sim 20$Å.

The elements of Equation 50 are susceptible to individual investigation. Measurements of the affinity of viscous binders, e.g., proteins, for calcium oxalate surfaces have been reported [58]. These measurements indicate that if the protein content of urine is 10 mg/dl, the surface of calcium oxalate particles will be covered more than 50% with adsorbed protein. Relating this observation to aggregation will require study of the effect of protein on aggregation kinetics. The electrostatic contribution of adhesion energy can be evaluated by study of the zeta potential of stone-salt precipitates. Figure 9 schematically shows the origin of zeta potential, and Figure 10 shows the effect of some urinary anions on zeta potential and the ease with which surface adsorption of the anions is demonstrated. The ability of our *ab initio* ion-equilibrium program to compute a two-phase equilibrium, given the total components of a system, makes it much easier to interpret zeta-

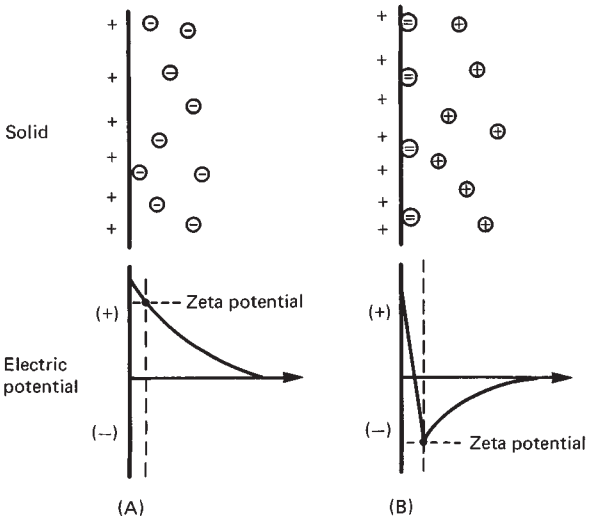

Fig. 9. *Zeta potential as an indicator for chemical adsorption of ions.* Whewellite is normally positively charged. **A)** In the absence of chemisorbed ions, a diffuse double layer of anions (−) exists and the zeta potential is positive. **B)** In the presence of chemisorbed anions ⊖, the net charge on the surface becomes negative and the counter ions ⊕ are cations. The *zeta potential* is a measure of the *electrical potential* between the layer of chemisorbed ions and the diffuse double layer of counter ions. The larger the extent of chemisorption, the more negative the zeta potential.

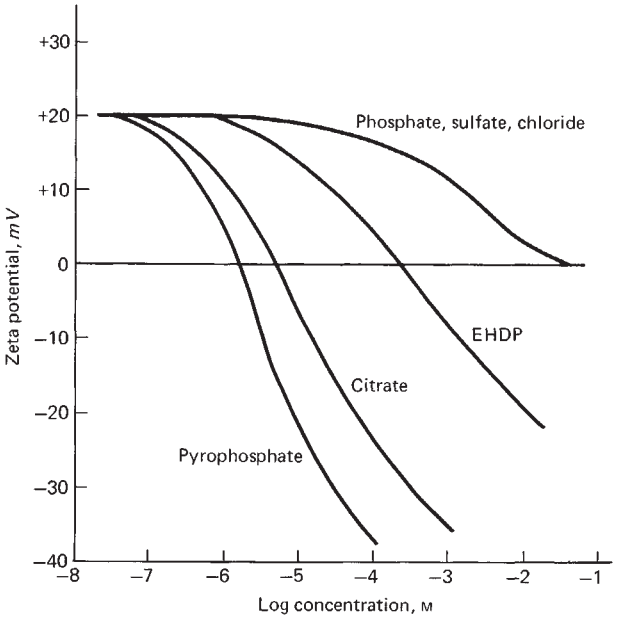

Fig. 10. *Effect of various ionic species on the zeta potential of whewellite.* The reversal of zeta potential by increasing amounts of pyrophosphate, citrate, and EHDP indicates the strong adsorbability of these ions. This effect may relate to the mechanisms of inhibition of polyvalent anions in urine. (Unpublished work by CURRERI, ONODA, and FINLAYSON.)

potential experiments. From the zeta potential, we can compute surface potential (ψ) with the Gouy-Chapman equation [59]. Because of the technical difficulty of measuring zeta potentials at ionic strength greater than 0.05, zeta potentials have yet to be measured in urine-like solutions. We anticipate doing it by a short extrapolative process. Van der Waal calculations for stone-salt particles have not been made.

It is appropriate to be skeptical about the importance of aggregation in urolithiasis or crystalluria. Robertson et al [8] have advanced the notion that aggregation inhibitors are important in urolithiasis. If aggregation occurs as a significant step in stone disease, it might be expected to occur in a manner somewhat like a Smoluchowski agglomeration [60], in which case,

$$N/N_0 = 1/(1 + (t/\tau)), \qquad (54)$$

in which N/N_0 is the fraction of particles remaining per unit volume after time (t) and τ is the time for $N/N_0 = \frac{1}{2}$, $\tau > 10^7/N_0$ if the unit of N_0 is particles/milliliter and the unit of τ is seconds [20]. Even if the 10^4 particles/ml in crystalluria reported by Robertson [32] is in error by two orders of magnitude, the expected aggregation would be so slow that one could not expect appreciable aggregation by a Smoluchowski process. This kinetic consideration, plus the small difference between the density of stones and the density of crystals, raises some doubt about the role of aggregation in urinary stone disease, and it is hoped that this important issue will receive more attention in the future.

Although lesions such as Randall's Plaques and encrusting cystitis require crystals to adhere to tissue, the energy of adherence has not been measured.

Inhibition of crystal growth and aggregation

A variety of molecules that occur in urine inhibit the crystal growth and aggregation of whewellite and apatite in simple solutions, e.g., pyrophosphate [61], nucleoside triphosphate [62], heparin, citrate, and EHDP [63]. As predicted by theory, zeta-potential measurement is a good screening process to look for surface-active urinary stone inhibitors. Whewellite zeta-potential perturbation by pyrophosphate behaves as expected (Fig. 10). Citric acid also shows, by zeta-potential perturbation, significant surface adsorption on whewellite (Fig. 10). Meyer and Smith [61] looked at inhibition of whewellite-seeded growth by citrate. By analysis of their rate-constant data, they concluded that citrate concentration for half-surface coverage of whewellite is 16 μM. This value has been confirmed in our laboratory by measuring adsorption isotherms. Meyer and Smith [61] concluded that the effect of citrate surface inhibition was small compared with complexing in solution. This may be incorrect for two reasons: Meyer and Smith did not account for the possibility that citrate causes the equilibrium concentration to be A_c, instead of A_0, and a Langmuir plot of their rate-constant data gives a negative intercept. Furthermore, the data in Figures 9 and 10 show a 39% inhibition of the growth rate by 50 μM citrate.

One of the major problems in evaluating urinary inhibitors is to know how they behave in urine. Current practice is to add an aliquot of urine to a seeded-growth system and observe its effect on crystal growth and aggregation [63]. This method does not necessarily indicate how the inhibitor works in undiluted urine. There can be profound dilutional effects. For example, the 100-fold dilution used by Robertson's group [64] will obscure the inhibitory effect of citrate and pyrophosphate that is expected on the basis of adsorption isotherm observations. The key to predicting inhibitor effects is the concentration necessary for half-surface coverage (this concentration is equivalent to a thermodynamic affinity). Another problem in evaluating the effect of inhibitors in urine is that the competitive effects of various urinary inhibitors are unknown. Nevertheless, Robertson et al [8] have exploited the dilution approach

to look at inhibition of calcium oxalate crystal growth and aggregation (termed "crystallization" by the Robertson group) by aliquots of urine in seeded supersaturated calcium oxalate solutions. They have found that stone-formers have less of a heparin-like inhibitor molecule in their urine than normal. A cluster analysis of the two variates, supersaturation and inhibitor concentration, readily separates stone-formers from non-stone-formers and has led them to formulate a saturation-inhibition index for classifying the predisposition of urine to form calcium oxalate stones. These workers have further observed that the effective concentration of heparin-like inhibitor in urine is a function of the total concentration of the inhibitor and the concentration of urate in urine [64].

There can be no doubt that crystal growth and aggregation inhibitors are present in urine; however, their role in the pathogenesis of stone disease is far from clear. Several causes of doubt about the role of aggregation in stone formation have already been cited. Another possibility is that the differences in urinary inhibitor concentration between stone-formers and normal subjects are a result of solution depletion by adsorption on crystalluria particles. Accordingly, inhibitor concentration becomes a correction on the estimate of supersaturation. This hypothesis could explain the apparent success of the saturation-inhibition index as well as the more obvious hypothesis of urinary inhibitors directly reducing crystallization activity in stone disease.

A final comment on the future of urolithiasis research

The last decade has seen a resurgence of interest in the physicochemical features of urolithiasis. During these years, techniques have been developed for evaluating ion equilibrium in complex urine-like solutions. The ability to calculate complex equilibria has put us in range of making penetrating studies of nucleation, crystal growth, and aggregation. Beyond these studies, we need to develop a valid understanding of the supersaturation and inhibitor-concentration profile along the nephron. We will then be able to start building a comprehensive kinetic picture of what can happen in urine as it moves through the urinary passages.

Acknowledgments

This work was supported by NIH grants AM-13023 and AM-20586. Figure 9 was prepared by Dr. George Y. Onoda.

Reprint requests to Dr. Birdwell Finlayson, Division of Urology, Department of Surgery, University of Florida, College of Medicine, Gainesville, Florida 32610, U.S.A.

References

1. NIELSEN AE: *Kinetics of Precipitation*. New York, Pergamon Press, 1964, p. 3
2. DAVIES CW: *Ion Association*. London, Butterworths, 1962
3. ROBINSON RA, STOKES RH: *Electrolyte Solutions*. London, Butterworths, 1959
4. ROBERTSON WG: Measurement of ionized calcium in biological fluids. *Clin Chim Acta* 24:149–157, 1969
5. PAK CYC, CHU S: A simple technique for the determination of urinary state of supersaturation for brushite. *Invest Urol* 11:211–215, 1972
6. GILL WB, SILVERT MA, ROMA MS: Supersaturation levels and crystallization rates of calcium oxalate from urines of normal humans and stone formers determined by a ^{14}C-oxalate technique. *Invest Urol* 12:203–209, 1974
7. FINLAYSON B: Calcium stones: Some physical and clinical aspects, Chapter 10, in *Calcium Metabolism in Renal Failure and Nephrolithiasis*, edited by DAVID DS, New York, John Wiley, 1977
8. ROBERTSON WG, PEACOCK M, MARSHALL RW, MARSHALL DH, NORDIN BEC: Saturation-inhibition index as a measure of the risk of calcium oxalate stone formation in the urinary tract. *N Engl J Med* 294:249–252, 1976
9. FINLAYSON B, SMITH A: Spectrophotometry of the stability constant of CaC_2O_4 based on competition between murexide and oxalate for Ca^{2+}. *J Eng Chem Data* 18:368–370, 1973
10. MARSHALL RW, ROBERTSON WG: Nomogram for the estimation of the saturation of urine with calcium oxalate, calcium phosphate, magnesium ammonium phosphate, uric acid, sodium acid urate, ammonium acid urate, and cystine. *Clin Chim Acta* 72:253–260, 1976
11. PAK CYC, HAYASHI Y, FINLAYSON B, CHU S: Estimation of the state of saturation of brushite and calcium oxalate in urine: A comparison of three methods. *J Clin Lab Invest* 89:891–901, 1977
12. PAK CYC, ARNOLD L, HOLT K, COX C, BARILLA D: Mechanisms for calcium urolithiasis among patients with hyperuricosuria. *J. Clin Invest* 59:426–431, 1973
13. SEARS GW: Influence of adsorbed films on crystal growth kinetics. *J Phys Chem* 25:154–159, 1958
14. OHATA M, PAK CYC: The effect of diphosphonate on calcium phosphate crystallization in urine in vitro. *Kidney Int* 4:401–406, 1973
15. PAK CYC, OHATA M, HOLT K: Effect of diphosphonate on crystallization of calcium oxalate in vitro. *Kidney Int* 7:154–160, 1975
16. ERWIN D, ROBERTS JA, SLEDGE G, BENNETT DJ, FINLAYSON B: Estimating urine supersaturation: A comparison of the result of two methods of evaluating changes induced by drinking milk, in *Urolithiasis Research*, edited by FLEISH H, ROBERTSON WG, SMITH LH, VAHLENSIECK W, New York, Plenum, 1976, pp. 261–264
17. PAK CYC: Quantitative assessment of various forms of therapy for nephrolithiasis in urinary calculi, in *Stone Research*, edited by CIFUENTES-DELATTE L, RAPADO A, Basal, Karger, 1972, pp. 177–187
18. BURDETTE WG, THOMAS WC, FINLAYSON B: Urinary supersaturation with calcium oxalate before and during orthophosphate therapy. *J Urol* 115:418–422, 1976
19. ROBERTSON WG, PEACOCK M, NORDIN BEC: Activity products in stone forming and non-stone forming urine. *Clin Sci* 34:579–594, 1968
20. WALTON AG: *The Formation and Properties of Precipitates*. New York, Interscience Publishers, 1961

21. Sears GW: The origin of spherulites. *J Phys Chem* 65:1738–1741, 1961.
22. Walton AG: Nucleation in liquids and solids, Chapter 5, in *Nucleation,* edited by Zottlemeyer AC, Marcel Decker, 1969
23. Turnbull D, Vonnegut B: Nucleation catalysis. *Indust Eng Chem* 44:1292–1298, 1952
24. Lonsdale K: Epitaxy as a growth factor in urinary calculi and gallstones. *Nature* 217:56–58, 1968
25. Venables JA, Price GL: Nucleation of thin films, in *Epitaxial Growth,* edited by Matthews JW, New York, Academic Press, 1975, p. 429
26. Murphy BT, Pyrah LH: The composition, structure and mechanisms of the formation of urinary calculi. *Br J Urol* 34:129–185, 1962
27. Keith HD, Padden FJ: A phenomenological theory of spherulitic crystallization. *J Appl Phys* 34:2409–2421, 1963
28. Uhlmann DR, Chalmers B: The energetics of nucleation. *Indust Eng Chem* 57:19–31, 1965
29. Garten VA, Head RB: Nucleation in salt solutions. *J Chem Soc [Perkin I]* 69:514–520, 1973
30. Robertson WG: A method for measuring calcium crystalluria. *Clin Chim Acta* 26:105–110, 1969
31. Johnson RT, Rousseau RW, McCabe WL: Factors affecting contact nucleation. *Am Inst Chem Eng Symposium Series* 68:31–41, 1972
32. DeBoer JH: *The Dynamical Character of Adsorption.* Oxford, The Clarendon Press, 1953, Chapter 1
33. Trump BF, Dees JH, Kim KM: Some aspects of kidney structure and function with comments on tissue calcification in the kidney, in *Urolithiasis,* edited by Finlayson B, Hench L, Smith LH, Washington, D.C., National Academy of Science, 1972, p. 1
34. Malek RS, Boyce WH: Intranephronic calculosis: Its significance and relationship to matrix nephrolithiasis. *J Urol* 109:551–555, 1973
35. Nielsen AE: The kinetics of electrolyte precipitation. *J Colloid Sci* 10:576–586, 1955
36. Coe FL, Lawton RL, Goldstein RB, Tembe V: Sodium urate accelerates precipitation of calcium oxalate in vitro. *Proc Soc Exp Biol Med* 149:926–929, 1975
37. Pak CYC, Hayashi Y, Arnold LH: Heterogeneous nucleation of calcium oxalate by seeds of monosodium urate. *Proc Soc Exp Biol Med* 149:930–932, 1975
38. Meyer J, Bergert J, Smith LH: Epitaxy in the calcium phosphate-calcium oxalate crystal growth systems, in *International Colloquium on Renal Lithiasis,* edited by Thomas WC, Finlayson B, Gainesville, Fla., University of Florida Press, 1976, pp. 66–76
39. Pak CYC, Hayashi Y, Arnold LH: Heterogeneous nucleation with urate, calcium phosphate and calcium oxalate. *Proc Soc Exp Biol Med* 153:83–87, 1976
40. Finlayson B, Miller GH: An analysis of experimental foreign body stone formation. *J Theor Biol* 23:344–346, 1969
41. Robertson WG, Peacock M, Nordin BEC: Calcium crystalluria in recurrent renal stone formers. *Lancet* 2:21–24, 1969
42. Doremus RH, Gardner GL, McKay W: Crystallization of calcium oxalate in various media and urolithasis, in *International Colloquium on Renal Stones,* edited by Thomas WC, Finlayson B, Gainesville, Fla., University of Florida Press, 1976, pp. 18–32
43. Nancollas GH, Gardner GL: Kinetics of crystal growth of calcium oxalate monohydrate. *J Cryst Growth* 21:267–276, 1974
44. Johnson RA, O'Rourke JD: The kinetics of precipitate formation: Barium sulfate. *J Am Chem Soc* 76:2124–2131, 1954
45. Füredi-Milhofer H, Purgaric B, Brecević L, Pavković N, Oljica E: Nucleation of calcium phosphate from solutions at physiological pH. *Croatica Chem Acta* 41:37–42, 1969
46. Marshall RW, Nancollas GH: The kinetics of crystal growth of dicalcium phosphate dihydrate. *J Phys Chem* 73:383–384, 1969
47. Meyer JL, Smith LH: Growth of calcium oxalate crystals: I. A model for urinary stone growth. *Invest Urol* 13:31–35, 1975
48. Finlayson B: Where and how does urinary stone disease start? An essay on the expectation of free-and-fixed particle urinary stone disease, in *International Bladder Stone Conference Proceedings,* Bethesda, Maryland, National Institutes of Health, Fogarty Center for International Studies, 1976, pp. 7–32.
49. Tomazic B, Nancollas GH: The seeded growth of calcium phosphates: Surface characterization and the effect of seed material. *J Coll Interface Sci* 50:451–461, 1975
50. Finlayson B: The concept of a continuous crystallizer. *Invest Urol* 9:258–263, 1972
51. Randolph AD, Larson MA: *Theory of Particulate Processes, Analysis and Techniques of Continuous Crystallization.* New York, Academic Press, 1971
52. Miller JD, Randolph AD, Drach GW: Some observations of calcium oxalate crystallization in urine-like mother liquors, in *International Colloquium on Renal Lithiasis,* edited by Thomas WC, Finlayson B, Gainesville, Fla., University of Florida Press, 1977, pp. 33–40
53. Miller JD: Crystallization kinetics of calcium oxalate in simulated urine. Ph.D. Thesis, University of Arizona, 1976
54. LeGeros R, Morales P: Renal stone crystals grown in gel systems. *Invest Urol* 11:12–16, 1973
55. Bisaillon S, Tawashi R: Growth of calcium oxalate in gel systems. *J Pharm Sci* 64:458–460, 1975
56. Rumpf H, Schubert H: Adhesion forces in agglomeration processes, in *Sciences of Ceramic Processing Before Firing,* edited by Onoda G, Hench L, New York, John Wiley and Sons Publishers, 1977
57. Meyer AS, Finlayson B, DuBois L: Direct observation of urinary stone ultrastructure. *Br J Urol* 43:154–163, 1971
58. Leal J, Finlayson B: Adsorption of naturally occurring polymers on calcium oxalate surfaces. *Invest Urol* 14:278–283, 1977
59. Adamson AW: *Physical Chemistry of Surfaces.* New York, Interscience Publishers, 1970
60. Overbeek JTG: Kinetics of flocculation, in *Colloid Science,* edited by Kyrut HR, Elsevier Press, 1952, pp. 278–301
61. Meyer JL, Smith LH: Growth of calcium oxalate crystals: II. Inhibition by natural urinary crystal growth inhibitors. *Invest Urol* 13:36–39, 1974
62. Meyer JL, McCall JT, Smith LH: Inhibition of calcium phosphate crystallization by nucleoside phosphates. *Calc Tiss Res* 15:287–293, 1974
63. Robertson WG, Peacock M, Nordin BEC: Inhibitors of the growth and aggregation of calcium oxalate crystals in vitro. *Clin Chim Acta* 43:31–37, 1973
64. Robertson WG, Knowles F, Peacock M: Urinary acid mucopolysaccharide inhibitors of calcium oxalate crystallization, in *Urolithiasis Research,* edited by Fleisch H, Robertson WG, Smith LH, Vahlensieck W, New York, Plenum Press, 1976